Enhancing the flame resistance of cotton by exploiting the interaction between calcium chloride and an aspartic acid-derived polyamidoamine

Jenny Alongi, Rony Aad, Paolo Ferruti, Elisabetta Ranucci

Dipartimento di Chimica, Università Degli Studi di Milano, Via C. Golgi 19, Milano, 20133, Italy. jenny.alongi@unimi.it (J.A.); rony.aad@studenti.unimi.it (R.A.); paolo.feruti@unimi.it (P.F.); elisabetta.ranucci@unimi.it (E.R.)

*** Corresponding author:** elisabetta.ranucci@unimi.it; Tel. +390250214132.

Abstract:

~~The recent finding that Ca^{2+} ions enhance the efficacy of the glycine-derived polyamidoamine M-GLY as a flame retardant for cotton prompted to study their effect in this respect of other α-amino acid-derived polyamidoamines.~~ In this work, the aspartic acid-derived polyamidoamine M-ASP, bearing two carboxyl group per repeat units, thus negatively charged at all pH's, was investigated. IR analysis confirmed that Ca^{2+} ions form Lewis's acid/base interactions with the amide groups of M-ASP. Their ionic interaction with the carboxylate pendants can reasonably be postulated. The effect of Ca^{2+} ions on the thermal and thermo-oxidative stability of cotton/M-ASP was superior to that of cotton/M-GLY, as demonstrated by thermogravimetric analysis. In horizontal flame spread tests, M-ASP/$CaCl_2$ protected cotton more efficiently than M-ASP. The effect of Ca^{2+} ions on cotton/M-ASP was greater than that of cotton/M-GLY, both in terms of higher final residue and reduced flaming and afterglow combustion times. In vertical flame spread tests, while M-ASP failed to stop cotton combustion, M-ASP/$CaCl_2$ coatings with add-ons 12% and 2%, respectively, inhibited cotton ignition, producing only modest afterglow, and leaving an almost intact mass. The effect was greater than that of M-GLY/$CaCl_2$ coatings, for which at least 19% M-GLY add-on was required. These findings demonstrate that the interaction of Ca^{2+} ions with the cotton/α-amino acid-derived polyamidoamine systems remarkably improves their flame retardancy, to an extent depending on the PAA chemical structure. Furthermore, it is evident that if on the one hand the hydrophilicity of PAAs derived from α-amino acids determines their easy washability, on the other hand it allows for the intimate interaction between cellulose and PAA. This suggests that, to ensure the durability of PAA coatings, it could be highly advantageous to covalently graft them onto cotton.

Keywords: cotton; polyamidoamines; aspartic acid; calcium chloride; synergism; flame retardancy.

1. Introduction

Fires represent one of the greatest risks to personal safety worldwide. The latest bulletin of the International Association of Fire Rescue and Services, published in 2022, reports that in the 33 countries surveyed calls to the fire brigade were 49 per 1,000 people in 2020, of which 1.1 due to fires and that in 2020 alone 4.0 million fires were reported, resulting in 20.7 thousand deaths. In addition, 24.2% of all fires that occurred were recorded in residential buildings (8.0%) and vehicles (11.5%), where flammable fabrics, mainly made of polyester and cotton, are widely used. It is known, in fact, that one of the most flammable fabrics is cotton, as it ignites easily and burns quickly (Speece 1974; Islam and van de Ven 2021). For this reason, both academic and industrial research have focused on the development of new high-performance flame-retardants (FRs) that can inhibit or delay the ignition of cotton (Ling et al. 2023).

Over the past 40 years, the most widely used durable FR formulations for cotton belong to two families of phosphorus products (Horrocks et al. 2005, Horrocks 2011), namely tetrakis(hydroxymethyl)phosphonium salts (Proban®) and N-methylalkylphosphonopropionamides (Pyrovatex®) (Diao et al. 2023). Even today, compounds containing phosphorus (Salmeia et al. 2016a) are considered among the most effective FRs for cotton. Indeed, alkyl phosphates (Salmeia et al. 2016b; Salmeia et al. 2016c; Tian et al. 1995, 2003), phosphonic acid derivatives (Sun et al. 2021a, 2021b; Xu et al. 2019), polyphosphoric acid derivatives (Horrocks 2011), phytic acid and phytic acid derivatives (Barbalini et al. 2020; Kang et al. 2022; Zilke et al. 2020) have been and are extensively studied. However, some of these FRs emit opaque fumes during combustion (Bourbigot et al. 2004) and can have a significant impact on human health and the environment due to release of formaldehyde during manufacturing and service life (Horrocks 2011). With these premises, non-toxic and environmentally friendly FRs would be very welcome by international regulations (Horrocks 2013).

It has long been known that the presence of inorganic salts or even of metal organic compounds modifies the thermal and thermo-oxidative decomposition pattern of cellulose (Cheng et al. 2013; Morterra and Low 1983, 1985; Patwardhan et al. 2010; Ponder et al. 1992; Sekiguchi et al. 1983; Sekiguchi and Shafizadeh 1984; Shafizadeh and Fu 1973; Shafizadeh and Sekiguchi 1983; Varhegyi et al. 1988; Yu 2013). Metal ions typically anticipate the onset of decomposition and maximum weight loss of cellulose and affect the nature and relative amount of its decomposition products. Thanks to their Lewis's acid nature, they stabilize specific reaction intermediates, thus favoring the dehydration of cellulose rather than its depolymerization (Sekiguchi and Shafizadeh 1984; Shafizadeh and Fu 1973) and giving rise to thermally stable aromatic chars (Ponder et al. 1992; Sekiguchi et al. 1983; Morterra and Low 1983, 1985). In this context, Ca^{2+} ions are no exception, thanks to their ability to interact with the hydroxyl groups of the glycosidic units of cellulose (Ponder et al. 1992).

Recently, flame-retardant nanocomposite coatings such as those obtained by combining in one case carbon black and carbon nanotubes with polyvinyl alcohol (Xia et al. 2022a), in a different case silver nanoparticles with a borate polymer (Xia et al. 2022b), have been used to produce multifunctional cotton fabrics. Their flame-retardant mechanism is explained by the ability of the nanofiller to accelerate carbonization and dehydration of the substrate.

Polyamidoamines (PAAs) are a family of linear polymers synthesized by the aza-Michael polyaddition of bis-acrylamides with bis-*sec*-amines or *prim*-amines, including among the latter naturally occurring α-amino acids (Ferruti 2013). Their polymerization processes are normally carried out in water at room temperature, under basic conditions and in the absence of added catalysts. Since it is a polyaddition reaction, no by-products are formed. Many PAAs derived from α-amino acids are biocompatible (Ferruti et al. 2002) and, in recent studies, some of them have been shown to be phytocompatible (Alongi et al. 2022). Numerous α-amino acid-derived PAAs have been shown to be considerably active as intumescent FRs for cotton (Alongi et al. 2023; Beduini et al. 2019, 2021; Forte et al. 2021; Manfredi et al. 2018). All were shown to be non-flammable in powder form, but capable of forming stable charry crusts which prevented the underlying powder from burning (Beduini et al. 2021; Forte et al. 2021). An in-depth study carried out by using Raman, X-ray photoelectron (XPS) and ^{13}C solid state nuclear magnetic resonance (NMR) spectroscopies was carried out on the glycine-derived PAA, encoded M-GLY taken as a model of α-amino acid-derived PAA flame-retardants (Forte et al. 2021). Raman spectroscopy provided evidence on the degree of graphitization of untreated and treated cotton char, whereas ^{13}C solid state nuclear magnetic resonance spectroscopy provided insight into the char structure, clearly indicating that M-GLY favors the carbonization of cotton and the formation of more highly condensed aromatic structures.

Preliminary unpublished TG/FT-IR studies carried out both in nitrogen and in air on PAAs show that they decompose on heating releasing non-flammable gases, including water, ammonia, and carbon dioxide, not carbon monoxide, not even in traces. Additionally, TG/FT-IR studies carried out in air on PAAs bearing two carboxyl functions per repeat unit showed that the carbon dioxide release was the most evident event, overshadowing all the others. TG/FT-IR studies carried out in air on cotton treated with M-GLY, taken as simple model of α-amino acid-derived PAA (Forte et al. 2021), showed that the PAA coating, though present at a low add-on, significantly enhanced the release of CO_2 and reduced the release of carbonyl compounds (namely, aldehydes and ketones), which represent combustible volatiles feeding the flame. This has been attributed to the fact that M-GLY promotes cellulose dehydration rather than depolymerization.

In oxygen-consumption cone calorimetry tests, α-amino acid-derived PAAs improved the resistance of cotton to a 35 kWm^{-2} irradiative heat flux, which is typical of fire developing step. They also

reduced the heat release rate peak, as well as the production of carbon oxides and smoke. In combustion tests, cotton strips impregnated with α-amino acid-derived PAAs with add-ons ranging from 4 to 7% inhibited or extinguished the flame in horizontal flame spread tests (HFSTs) (Manfredi et al. 2018). Only the cystine-based polymer M-CYSS and the glycine/cystine copolymers have proven capable to extinguish the flame even in the severe vertical flame spread tests (VFSTs) (Beduini et al. 2019).

The presence of small amounts of Ca^{2+} ions was recently shown to significantly enhance the efficacy of the PAA encoded M-GLY as a flame-retardant of cotton (Alongi et al. 2023). Thermogravimetric analysis demonstrated superior thermo-oxidative stability of cotton treated with M-GLY/$CaCl_2$ blends compared to cotton treated separately with either M-GLY or $CaCl_2$ above 350°C, suggesting that they act synergistically. In HFST, M-GLY/$CaCl_2$ coatings were even more efficient than the M-GLY coatings and showed lower flaming and afterglow times at the same M-GLY add-on. In VFSTs, M-GLY/$CaCl_2$ coatings with add-ons 19% and 2%, respectively, inhibited the ignition of cotton, producing only a modest afterglow and leaving 82% residue. It should be noted that, in VFSTs, M-GLY alone did not protect cotton even with >30% add-ons. The synergistic activity of Ca^{2+} ions and M-GLY has been explained by two concurring interactions. Ca^{2+} ions can, indeed, give rise to both ionic exchange equilibrium with the carboxylate pendants and Lewis's acid/base interactions with the amide C=O of M-GLY.

Considering the positive effect of Ca^{2+} ions on M-GLY activity, it was considered interesting to investigate whether Ca^{2+} ions promoted a synergistic flame-retardant activity even when combined with other α-amino acid-derived PAAs. In particular, the performances as flame-retardants for cotton of M-ASP/$CaCl_2$ formulations in which the polymeric component was the aspartic acid-derived PAA M-ASP, bearing in its repeat unit one additional carboxyl group with respect to M-GLY, were studied. The aim of this paper is to report on the obtained results.

2. Materials and Methods

2.1 Materials

Aspartic acid (ASP, >98%), *N,N′*-methylenebisacrylamide (99%), lithium hydroxide monohydrate ($LiOH{\cdot}H_2O$, 98%), calcium chloride ($CaCl_2$, >97%), hydrochloric acid (37% aqueous solution) and D_2O and DCl (99.9%) were purchased from Sigma-Aldrich (Milano, Italy) and used as received. Aqueous solutions were prepared using deionized water obtained with a Q20 Millipore system. Cotton fabric (COT) having an area density of 200 gm^{-2} was purchased from Fratelli Ballesio S.r.l. (Torino, Italy).

2.2 Characterization techniques

The ^{1}H-nuclear magnetic resonance (^{1}H-NMR) spectra of PAAs were obtained in D_2O at 25 °C using a Bruker Avance DPX-400 NMR spectrometer operating at 400.13 MHz. The thermal and thermal oxidative stability of PAAs, PAA-treated and PAA-Ca^{2+}-treated cotton fabrics were evaluated by thermogravimetric analysis (TGA) in nitrogen and air from 50 to 800 °C with a heating rate 10 °C min^{-1}. To this aim, a Perkin Elmer thermogravimetric balance, TGA 7 - Thermogravimetric Analyzer model, was used, placing samples (5 mg for both powders and textiles) in open platinum pans, in either inert or oxidative atmosphere, 20 mL min^{-1} gas flow (Perkin Elmer, Milano, Italy). The surface morphology of untreated, PAA-treated and PAA-Ca^{2+}-treated cotton fabrics, and combustion residues was characterized using an EVO 15 equipped with a ULTIM MAX 40 probe scanning electron microscope (SEM) (Zeiss, Ramsey, NJ, USA), operating at 8.5 mm working distance, under 5 kV beam voltage, equipped with Energy-Dispersive X-ray Spectroscopy (EDX, Jena, Germany) to perform elemental analyses. Fabric pieces (5 mm x 5 mm) or combustion residues were fixed to sample holder through conductive adhesive tapes and gold metalized.

2.3 Synthesis of M-ASP

M-ASP was synthesized as already reported (Beduini et al. 2021). Briefly, *N,N′*-methylenebisacrylamide (MBA, 4.65 g; 0.03 mol), aspartic acid (4.10 g; 0.03 mol), and lithium hydroxide monohydrate (2.57 g; 0.06 mol) were suspended in water (17.0 mL). The reaction mixture was heated to 50-55 °C until complete dissolution of MBA and then left for 5 days at 25 °C in the dark. It was then diluted to 25 mL with water, and the pH adjusted to 4.5 with 37% hydrochloric acid. The final product was retrieved by freeze-drying the retained portion. The yield was nearly quantitative. The chemical structure of M-ASP was confirmed by ^{1}H-NMR and FT-IR/ATR spectroscopies (Figures S1 andS2, respectively, in Supplementary Information).

2.4 Impregnation of cotton fabrics

Before impregnation, 40 mm x 80 mm strips of cotton fabrics were dried for 4 min at 110 °C, then weighed after 10 min at room temperature until constant weight.

M-ASP-coated cotton strips (COT/M-ASP) were obtained by impregnating twice the dried cotton strips with an aqueous solution with known M-ASP concentration. The cotton strips were coated by uniformly wetting them with known aliquots of the M-ASP solution added in sequence (10 × 200 μL), then drying them for 4 min at 110 °C, and finally weighing them. The concentration of the impregnating M-ASP solution was 3.5 wt.-%.

The total dry, solid add-ons (*Add-on, wt.%*) were determined by weighing each sample before (W_i) and after drying that follows the impregnation (W_f). The add-ons were calculated using Equation (1):

$$Add - on = \frac{W_f - W_i}{W_i} \times 100 \qquad \text{Equation (1)}$$

The final add-ons for M-ASP treated fabrics were 7% for horizontal flame spread tests and 12% for vertical flame spread tests, by using 3.5 wt.-% and 5.5 wt.-% M-ASP solution concentrations. The add-ons selected for vertical flame spread tests were higher to those adopted in horizontal configuration, since the vertical configuration represents a more severe fire scenario, being the combustion forced by the chimney effect.

$CaCl_2$-coated cotton strips (COT-Ca^{2+}) with add-on 2% were obtained by impregnating once the dried cotton strips with a 2 wt.% $CaCl_2$ aqueous solution.

Cotton fabrics impregnated with both M-ASP and $CaCl_2$ (COT/M-ASP-Ca^{2+}) were obtained adopting by first impregnating the cotton strips with $CaCl_2$ and then with M-ASP following the above-described procedures.

The chemical structure of COT/M-ASP, COT-Ca^{2+} and COT/M-ASP-Ca^{2+} was confirmed by FT-IR/ATR spectroscopy (Figures S3).

2.5 Combustion tests

The ignitability of M-ASP was determined by applying a butane flame of 20 mm length for 20 s to freeze-dried powdered polymer samples (350 mg) placed on a square piece of glass. The ignitability of M-ASP/$CaCl_2$ mixtures (350 mg M-ASP and 25 mg $CaCl_2$) was determined following the same procedure. The M-ASP/$CaCl_2$ mixtures were obtained by grinding together the two components in a pestle and mortar to ensure homogenous dispersions. Before testing, the specimens were conditioned at 27 ± 1 °C and 50% relative humidity in a climate chamber until constant weight. All experiments were performed in duplicate.

Combustion flame spread tests were carried out in horizontal and vertical configurations on 40 mm x 80 mm rectangular specimens placed in a metal frame. In those for horizontal spread tests (HFSTs) the shorter side of the specimen was tilted by 45° with respect to the vertical axis. In all tests, the specimens were exposed to a butane flame (20 mm length), for 3 s in the horizontal configuration, and 2 s in the vertical configuration. All tests were repeated in sextuplicate. Flaming combustion time (s), afterglow combustion time (s) and residual mass fraction (RMF, wt.-%) were assessed and

compared with those of untreated cotton. The duration of flame application as well as the combustion times were determined by analyzing the videos of the experiments.

The resistance to an irradiative heat flux of 100 mm x 100 mm x 2 mm square fabrics was investigated by using an oxygen-consumption cone calorimeter (Noselab, ats-fire testing, Monza-Brianza, Italy). Measurements were carried placing samples in horizontal configuration under 35 kW m^{-2} heat flux, following a procedure previously reported (Tata et al. 2011), optimized based on the ISO 5660 standard (2002). Parameters such as the time to ignition (TTI, s), heat release rate peak (pkHRR, kW m^{-2}), total heat release (THR, MJ m^{-2}), and residual mass fraction (RMF, wt.%) were determined. Prior to the combustion tests, all specimens were conditioned to constant weight at 23 ± 1 °C for 48 h at 50% relative humidity in a climatic chamber. Each experiment was performed in triplicate and the mean standard deviation was calculated.

3. Results

3.1 Rationale

As already stated in Introduction, it is known that the effect of Ca^{2+} ions on the thermal and thermo-oxidative stability of cellulose is due to their strength as Lewis's acids. This allows Ca^{2+} ions to interact with the hydroxyl groups of the pyranose rings, promoting the homolytic cleavage of ring covalent bonds (Patwardhan et al. 2010) (Figure 1). This, in turn, favors dehydration reaction rather than depolymerization (Sekiguchi and Shafizadeh 1984; Shafizadeh and Fu 1973), and the formation of thermally stable aromatic char (Ponder et al. 1992; Sekiguchi et al. 1983; Morterra and Low 1983, 1985).

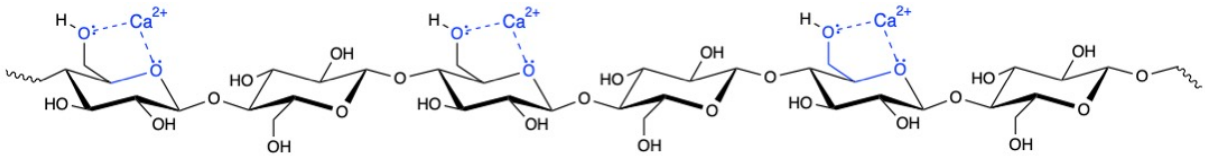

Figure 1. Interaction of cellulose with Ca^{2+} ions (Patwardhan et al. 2010).

As already commented on in the case of M-GLY (Alongi et al. 2023), Ca^{2+} ions interact with the repeat units of M-ASP, whose structure is shown in Figure 2a, in different ways. In particular, ionic interactions and Lewis's acid/base interactions may occur (Figure 3).

Concerning the ionic species distribution of M-ASP it should be observed that its repeat units exhibit three ionizable functions, namely a tert-amine function with pK_{a1} 7.40, and two carboxyl pendants with pK_{a2} 3.37 and pK_{a3} 1.85, respectively. M-ASP pK_a values were determined from the half-equivalence points, where pH = pK_a, as detected in the forward potentiometric titration (Figure S4a). Since

M-ASP was deposited on cotton at pH 3.5, the tert-amino groups in the backbone were 100% protonated, one of the carboxyl pendants was completely deprotonated, while the second carboxyl pendant was approximately 50% deprotonated. Thus, the net average charge of the M-ASP repeat units is negative, which allows for their ionic interaction with Ca^{2+} ions (Figure 2b).

Furthermore, Lewis's acid/base interactions can occur between Ca^{2+} ions and amide carbonyl groups (Figures 3a-3c) (see section 3.2), in line with what has already been postulated for M-GLY (Alongi et al. 2023). Ca^{2+} ions can also act as a bridge between cellulose and M-ASP repeat units, by means of ionic and Lewis's acid/base interactions (Figure 3d).

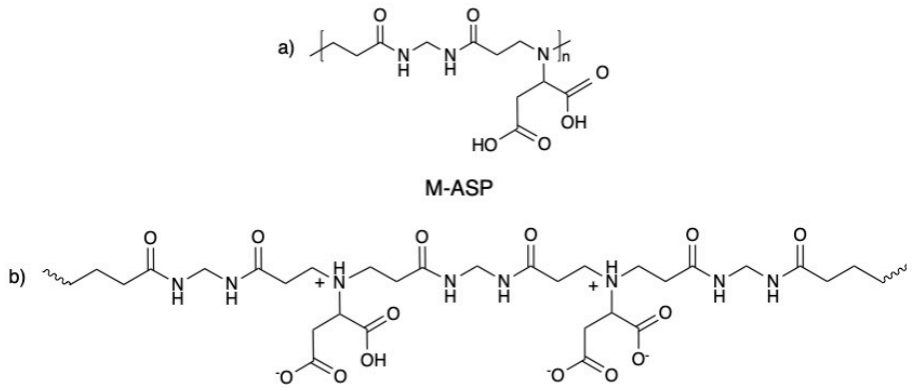

Figure 2. M-ASP repeat unit: structure (**a**) and pH-dependent ionic species distribution (**b**).

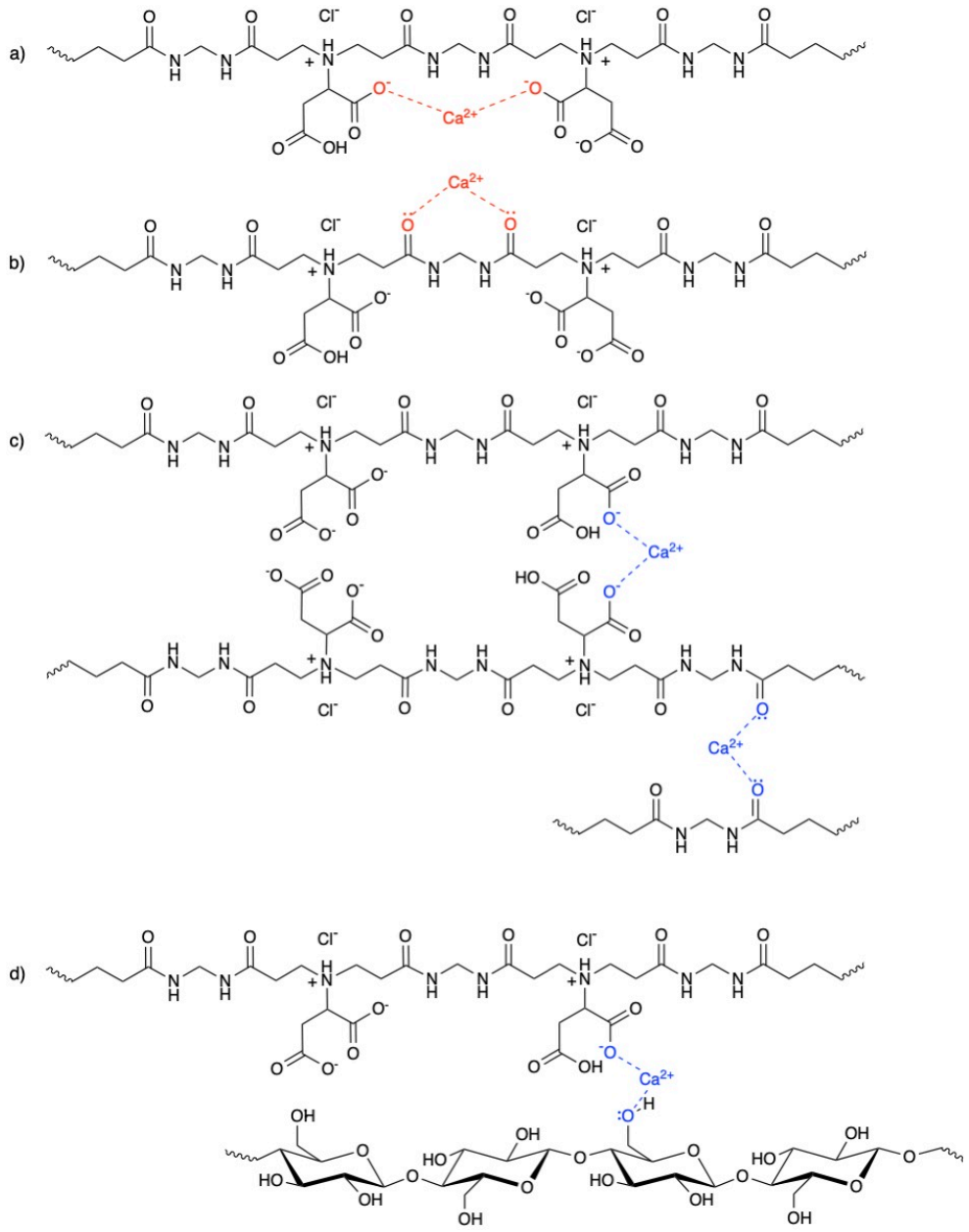

Figure 3. Examples of possible intramolecular and intermolecular ionic and Lewis's acid/base interactions of Ca^{2+} ions with the repeat units of M-ASP and cellulose: intramolecular M-ASP/Ca^{2+} interactions (in red **a,b**); intermolecular M-ASP/Ca^{2+} interactions (in blue **c**); intermolecular M-ASP/Ca^{2+}/cellulose interactions (in blue **d**).

3.2 Synthesis of the aspartic acid-derived polyamidoamine M-ASP

M-ASP was synthesized following an already reported procedure by the aza-Michael polyaddition of *N,N′*-methylenebisacrylamide (MBA) with aspartic acid in a 1:1 molar ratio (Scheme 1) (Beduini et al. 2021). M-ASP was prepared in a single step in water at pH 10.5 and a 40 wt.% concentration. The reaction mixture gradually became homogeneous and, after being left to rest under occasional stirring at 25°C for 5 days, was freeze-dried. The products were used with no further purification. The

chemical structure of M-ASP was confirmed by ^{1}H-NMR and FT-IR/ATR spectroscopies (Figures S1 and S2, respectively). The number average molecular weight was calculated from the ^{1}H-NMR spectrum from the ratio between the integrals of the resonance peaks relative to the terminal units and the integrals of the resonance peaks relative to the internal repeat units. The spectrum of M-ASP was consistent with an oligomer with molecular weight 3500.

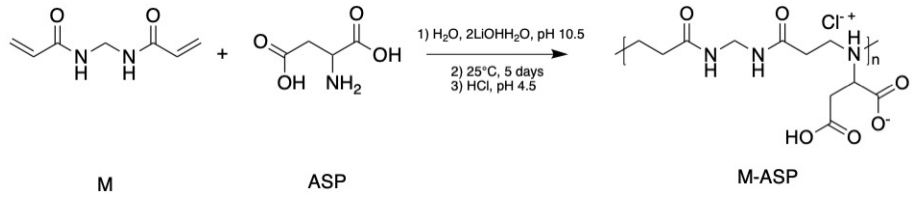

Scheme 1. Synthesis of M-ASP.

The interaction mode of Ca^{2+} ions with the repeat units of M-ASP was studied by comparing the FT-IR/ATR spectrum of M-ASP with that of a 3.5:1 (on a weight basis) M-ASP/$CaCl_2$ mixture, corresponding to the weight ratio found in the flame-retardant formulation adopted in this study in horizontal flame spread tests. This comparison is shown in Figure S2. The M-ASP spectrum has two diagnostic peaks placed at 1628 and 1546 cm^{-1}. The first peak is due to the overlapping of the carboxylate stretching and the amide I bands, while the second peak corresponds to the amide II band, namely, the amide N-H bending. In the M-ASP-Ca^{2+} mixture, the N-H bending band has significantly reduced, suggesting the occurrence of Ca^{2+}/amide C=O groups interactions, which affects the H-bond strength involving the amide N-H, and causes the band shift to higher wavenumbers. This effect, also observed for M-GLY-Ca^{2+} (Alongi et al. 2023), has been already reported for polyamide 6,6 (Rietzler et al. 2021).

3.3 Comparison between the thermal stability of M-ASP-Ca^{2+} and M-ASP

Figure 4 shows the thermogravimetric curves (TG) and their first derivative (dTG) of M-ASP-Ca^{2+} and M-ASP in nitrogen (Figures 4a and 4c) and air (Figures 4b and 4d) in the 50 - 800 °C range. The thermal data collected are shown in Table 1. The M-ASP-Ca^{2+} sample was obtained by preparing first a solution of M-ASP with $CaCl_2$ in a 3.5:1 weight/weight ratio in water and then freeze-drying it, thus achieving a homogeneous solid mixture. The M-ASP/$CaCl_2$ weight ratio was the same used for impregnating cotton samples tested in horizontal flame spread tests. The weight loss of M-ASP-Ca^{2+} shown in Figure 4 from 100°C to 150°C is due to sample drying. This phenomenon is commonplace in highly hydrophilic polymers such as PAAs.

Overall, the collected data indicate that the presence of Ca^{2+} remarkably anticipates both the thermal and thermo-oxidative decomposition of M-ASP, as clearly shown by the shift of the TG thermograms

towards lower temperature values in the 50-350 °C range (Figures 4a and 4b and $T_{onset10\%}$ and T_{max1} values in Table 1). In nitrogen (Figure 4a), the presence of Ca^{2+} leads to the formation of a higher amount of char in the 350-400 °C range and to a higher residual mass fraction at 800 °C. The RMF_{800} values were indeed 15.0% *vs*. 40.0% for M-ASP and M-ASP-Ca^{2+}. The RMF_{800} of M-ASP-Ca^{2+} includes a 2% $CaCl_2$ residue (Table 1).

In air (Figure 4b) M-ASP and M-ASP-Ca^{2+}decomposition occurred through a complex mechanism, and once again the presence of Ca^{2+} favored the formation of a thermally stable char due to the intumescent character of PAAs in between 300-500 °C (Manfredi et al. 2018; Forte et al. 2021). In the case of M-ASP-Ca^{2+}, this char partially oxidized at higher temperatures leaving 24% RMF_{800} (including a 2% $CaCl_2$ residue), whereas in the case M-ASP oxidation was complete and RMF_{800} approached 0%. This peculiar result clearly reveals the existence of synergism between M-ASP and Ca^{2+} ions, confirming the hypothesis postulated in this work of the occurrence of strong interactions among them (Figures 3a and 3c).

A similar effect of Ca^{2+} ions was also observed in the case of M-GLY (Alongi et al. 2023). However, by comparing the RMF_{800} values both in nitrogen and air, it apparent that the effect on the M-ASP is remarkably higher than in M-GLY (RMF_{800} in nitrogen 20% and 37% for M-GLY and M-GLY-Ca^{2+}; RMF_{800} in air 0% and 19% for M-GLY and M-GLY-Ca^{2+}). This result can clearly be ascribed to the difference in the structural features of M-ASP and M-GLY repeat units. In particular, the presence in M-ASP of a second carboxyl pendant increases the density of negatively charged species facilitating the interaction with Ca^{2+} ions.

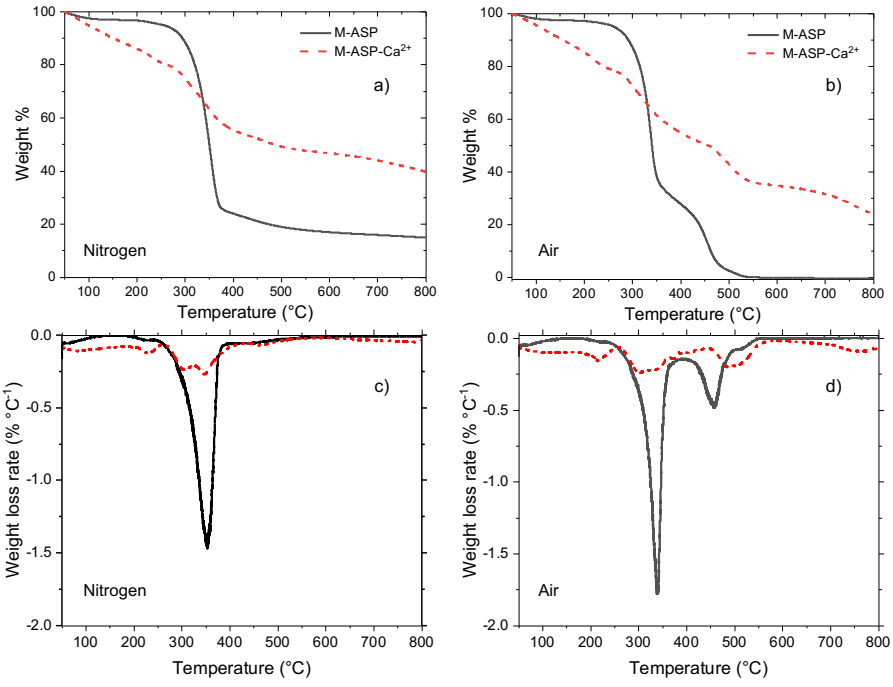

Figure 4. TG and dTG thermograms of M-ASP in nitrogen (**a** and **c,** respectively) and air (**b** and **d**, respectively). The 3.5:1 M-ASP/$CaCl_2$ ratio (w/w) in M-ASP-Ca^{2+} is the same used in HFSTs.

Table 1. Thermal data of M-ASP and M-ASP-Ca^{2+} in nitrogen and air by thermogravimetric analysis.

Sample	$T_{onset10\%}$ [a] (°C)	T_{max1} [b] (°C)	T_{max2} [c] (°C)	RMF_{800} [d] (%)
		Nitrogen		
M-ASP	294	354	-	15.0
M-ASP-Ca^{2+} [e]	149 [f]	309/345	-	40.0 [g]
		Air		
M-ASP	291	340	458	0
M-ASP-Ca^{2+} [e]	155 [f]	304/333	487	24.0 [g]

[a] Onset decomposition temperature at 10% weight loss. [b] First temperature at maximum weight loss rate obtained from the derivative thermogravimetric curve (Figures 4c and 4d). [c] Second temperature at maximum weight loss rate obtained from the derivative thermogravimetric curve (Figure 4d). [d] Residual mass fraction at 800 °C. [e] 3.5:1 M-ASP/$CaCl_2$ ratio (w/w). [f] This value is affected by the weight loss due to sample drying. [g] This value includes a 2% $CaCl_2$ residue.

3.4 Ignitability of M-ASP-Ca^{2+}

The ignitability of M-ASP-Ca^{2+} was evaluated by exposing the surface of a mound of a homogeneous mixture of M-ASP/$CaCl_2$ (350 mg M-ASP and 25 mg $CaCl_2$) to a butane flame for 30 s. After this time, the initially white powder was covered with a hard carbonaceous coating (char). Results were compared with those obtained with an M-ASP powder sample of the same size (Figure 5). No significant differences were observed in the char thickness formed on both M-ASP-Ca^{2+} and M-ASP samples (1-2 mm), as well as on the residual mass fraction, approaching 98-99% in both cases.

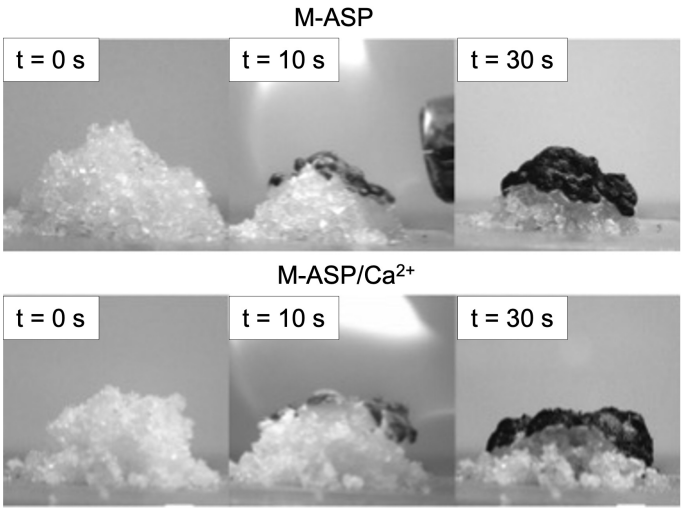

Figure 5. Snapshots of ignitability tests of M-ASP-Ca^{2+} and M-ASP.

3.5 *Effect of Ca^{2+} ions on the thermal stability of M-ASP-treated cotton fabrics*

The TG and dTG thermograms of M-ASP-Ca^{2+}-treated cotton in nitrogen and in air in the 50-800 °C range are shown in Figure 6. For comparison purposes, the TG thermograms of M-ASP-treated cotton and untreated cotton obtained in the same conditions are shown in the same figure. The thermal data are summarized in Table 2. Overall, in both nitrogen and air $CaCl_2$, M-ASP and M-ASP-Ca^{2+} sensitized the thermal decomposition of cotton (Figure 6), as evidenced by the significant reduction of the $T_{onset10\%}$ values (Table 2) (Davies et al. 2005). In nitrogen, after the first weight loss, untreated cotton left approximately 10% residue, to be compared with a 25-35% residue for M-ASP- and Ca^{2+}-treated cotton (Figure 6a). These residues further decomposed at higher temperatures but leaving a higher RMF_{800} with respect to that left by cotton; in fact, the RMF_{800} of COT/M-ASP-Ca^{2+} is significantly higher than that of COT/M-ASP: 24.5% *vs*. 15.0% (Table 2).

In air, the thermal stability of COT/Ca^{2+}, COT/M-ASP and COT/M-ASP-Ca^{2+} was much higher than that of untreated cotton, particularly in 350-650 °C range, where M-ASP underwent intumescence (Figure 6b). Above 500 °C the residual mass of COT/M-ASP-Ca^{2+} (approximately 30%, including 2% $CaCl_2$) was much higher than the sum of those of COT/Ca^{2+} and COT/M-ASP (5% and 2%, respectively), clearly indicating that M-ASP and $CaCl_2$ synergically protect cotton from thermal oxidation. This behavior can be ascribed to intramolecular and intermolecular ionic and Lewis's acid/base interactions between M-ASP and Ca^{2+} (Figures 3a-3c) and to the occurrence intermolecular cellulose/Ca^{2+}/M-ASP interactions (Figure 3d).

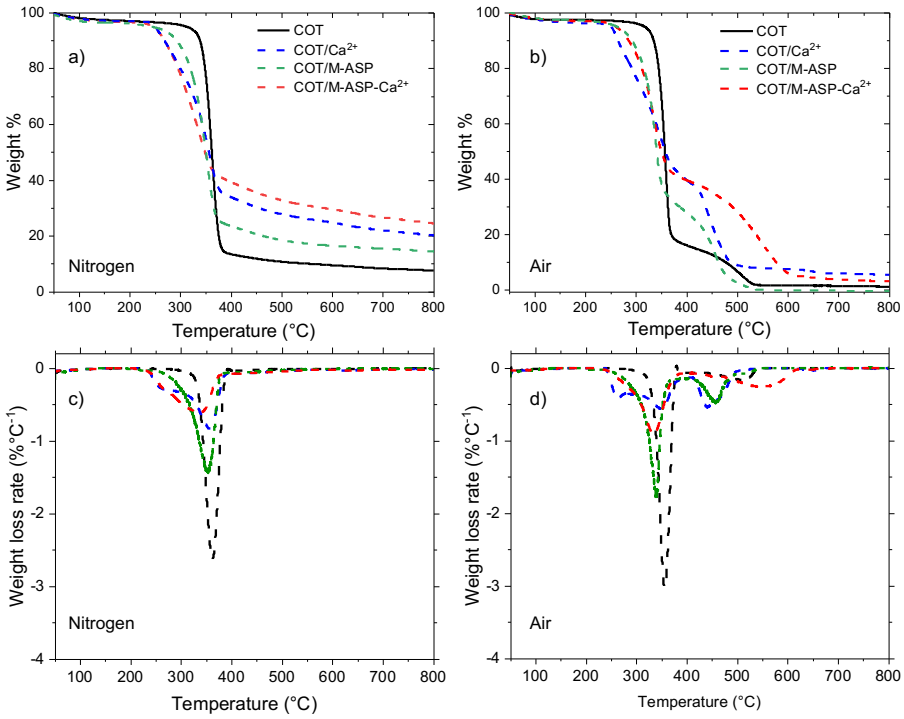

Figure 6. TG and dTG thermograms of: COT/M-ASP and COT/M-ASP-Ca^{2+} in nitrogen (**a** and **c**, respectively) and air (**b** and **d**, respectively); COT/Ca^{2+} add-on: 2%. COT/M-ASP add-on: 7%. COT/M-ASP-Ca^{2+} add-on: 2% $CaCl_2$ and 7% M-ASP.

Table 2. Thermal data of M-ASP and M-ASP-Ca^{2+}-treated cotton fabrics in nitrogen and air by thermogravimetric analysis.

Sample	$T_{onset10\%}$ [a] (°C)	T_{max1} [b] (°C)	T_{max2} [c] (°C)	RMF_{800} [d] (%)
Nitrogen				
COT	339	363	-	7.5
COT/Ca^{2+} [e]	268	359	-	20.0
COT/M-ASP [f]	292	354	-	15.0
COT/M-ASP-Ca^{2+} [g]	268	339	-	24.5 [h]
Air				
COT	335	357	511	0
COT/Ca^{2+} [e]	264	352	440	4.0
COT/M-ASP [f]	292	339	460	0
COT/M-ASP-Ca^{2+} [g]	285	335	558	3.0 [h]

[a] Onset decomposition temperature at 10% weight loss. [b] First temperature at maximum weight loss rate obtained from the derivative thermogravimetric curve (Figures 6c and 6d). [c] Second temperature at maximum weight loss rate obtained from the derivative thermogravimetric curve (Figure 6d). [d] Residual mass fraction at 800 °C. [e] COT/Ca^{2+} add-on: 2%. [f] COT/M-ASP add-on: 7%. [g] COT/M-ASP-Ca^{2+} add-on: 2% $CaCl_2$ and 7% M-ASP. [h] This value includes a 2% $CaCl_2$ residue.

3.6 Morphological characterization of M-ASP-Ca^{2+}-treated cotton fabrics

The surface morphologies of cotton fabrics impregnated with M-ASP and M-ASP-Ca^{2+}, whose structures have been confirmed by FT-IR/ATR (Figure S3), were assessed by SEM observations. The SEM micrographs of untreated cotton, of cotton treated with M-ASP and M-ASP-Ca^{2+} are shown in Figure 7. Both untreated and M-ASP-treated cotton fabrics showed fibers characterized by smooth, flat surfaces that retained their discreteness. In case of M-ASP-Ca^{2+}, the fiber surfaces appeared rougher due to the coating (Figures 7c,7d and 7e,7f for M-ASP and M-ASP-Ca^{2+}, respectively). Despite the very low add-on, the distribution of Ca^{2+} on treated cotton fabrics was found to be fine and homogeneous, as confirmed by the EDX analysis. In Figure 8, the mapping of C, O, and Ca elements of M-ASP-Ca^{2+} was reported.

Furthermore, it should be noted that, thanks to their high-water solubility, all α-amino acid-derived polyamidoamines, including M-ASP, so far investigated as flame-retardants for cotton, have a high affinity for cotton, thus intimately impregnating cotton fibers, penetrating inside them (Beduini et al. 2021) and generating a very thin layer on cotton surface that is barely visible even by SEM analysis. Only with very high PAA coating add-ons, above 20%, does the hand of the fabrics change

significantly, making them slightly stiffer. On the contrary, in this study, the COT/M-ASP-Ca^{2+} samples have low add-ons, namely, 7-10% M-ASP and 2% $CaCl_2$, and therefore are soft, pleasant to the touch and do not noticeably change the hand of the fabrics than that of untreated cotton.

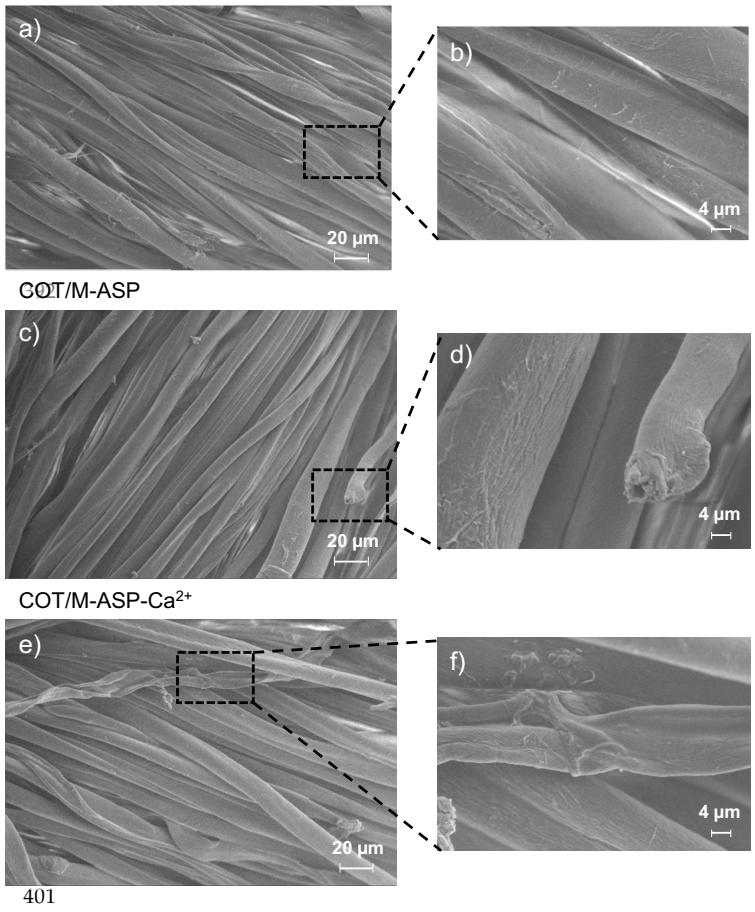

Figure 7. SEM micrographs at different magnifications of: untreated cotton fabrics (**a,b**); cotton fabrics treated with M-ASP (**c,d**), and M-ASP-Ca^{2+} (**e,f**). COT/M-ASP add-on: 7%. COT/M-ASP-Ca^{2+} add-on: 2% $CaCl_2$ and 7% M-ASP.

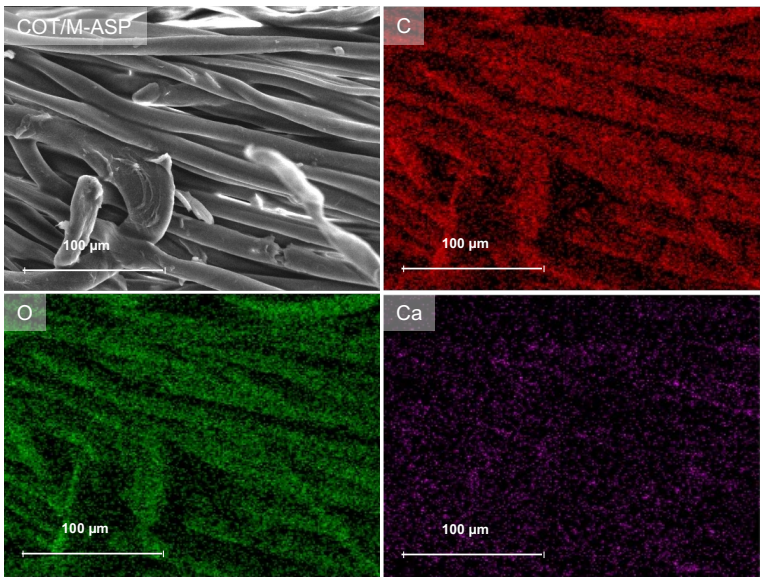

Figure 8. EDX analysis of COT/M-ASP-Ca^{2+} sample whose morphology is shown in Figure 7. Distribution of carbon (C), oxygen (O), and calcium (Ca) elements.

3.7 Combustion of M-ASP-Ca^{2+}-treated cotton fabrics

3.7.1 Horizontal Flame Spread Tests (HFSTs)

The combustion behavior of M-ASP-Ca^{2+}-treated cotton fabrics was first studied by horizontal flame spread tests and compared with that of M-ASP-treated cotton fabrics and untreated cotton. Snapshots taken at the beginning and the end of the combustion are shown in Figure 9; relevant combustion data are listed in Table 3. Cotton (COT) burned slowly in the presence of flame for 80 s and then when the flame-out was reached, the unburned area was almost totally consumed due to afterglow lasting 35 s (Figure 9). As already observed (Alongi et al. 2023), $CaCl_2$ alone did not modify cotton behavior. Regarding M-ASP, the minimum add-on useful for reaching the self-extinguishment was 7% in line with the results of a previous work (Beduini et al. 2021). In fact, at this add-on, COT/M-ASP burned for only 17 s in the presence of flame and after 68 s afterglow reached self-extinguishment, consuming a very limited area (Figure 9), and leaving an RMF 90% (Table 3). The combination of M-ASP with $CaCl_2$ was significantly more effective than M-ASP alone since cotton treated with M-ASP-Ca^{2+} burned for few seconds, only 3 s, and after 18 s afterglow left a residue higher than that left by M-ASP: 99% *vs*. 90% for M-ASP-Ca^{2+} and M-ASP, respectively (Table 3).

It is reasonable to assume that this improvement was achieved thanks to the intramolecular and intermolecular ionic and Lewis's acid/base interactions of Ca^{2+} ions with the repeat units of M-ASP (Figures 3a-3c) that allow Ca^{2+} ions catalyze the PAA cyclization reaction which induces the formation of char. Analogously, thanks to the possible intermolecular interactions M-ASP/Ca^{2+}/cellulose interactions (Figure 3d), Ca^{2+} ions can catalyze the dehydration reaction of cellulose to form char, instead of depolymerization.

Furthermore, it was observed that the effect of Ca^{2+} ions on the flame-retardant activity of M-ASP was higher than that of M-GLY, as clearly evidenced by comparing the combustion times (10 s *vs.* 3 s as flaming combustion time and 51 s *vs.* 18 s afterglow combustion time for M-ASP-Ca^{2+} and M-GLY-Ca^{2+}, respectively) and final RMF values (99% *vs.* 90% for M-ASP-Ca^{2+} and M-GLY-Ca^{2+}, respectively).

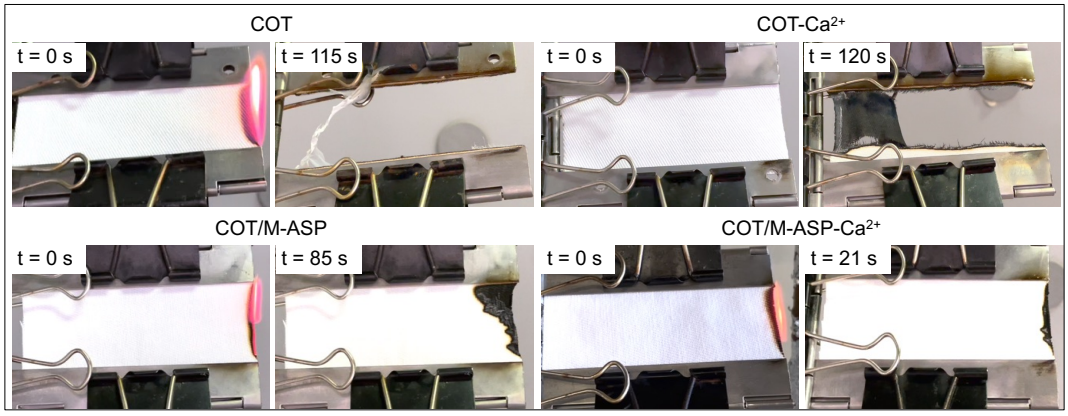

Figure 9. Snapshots of horizontal flame spread tests for untreated cotton and cotton treated with Ca^{2+}, M-ASP, and M-ASP-Ca^{2+}. COT/Ca^{2+} add-on: 2%. COT/M-ASP add-on: 7%. COT/M-ASP-Ca^{2+} add-on: 2% $CaCl_2$ and 7% M-ASP.

Table 3. Combustion data of M-ASP and M-ASP-Ca^{2+}-treated cotton fabrics from horizontal flame spread tests.

Sample	**Flaming combustion time [a] (s)**	**Afterglow combustion time [a] (s)**	**Extinguishment**	**RMF [b] (%)**
COT	80	35	NO	<1
COT-Ca^{2+} [c]	85	35	NO	16
COT/M-ASP [d]	17	68	YES	90
COT/M-ASP-Ca^{2+} [e]	3	18	YES	99

[a] Combustion time ± 1 s. [b] RMF ± 1.0%. [c] COT/Ca^{2+} add-on: 2%. [d] COT/M-ASP add-on: 7%. [e] COT/M-ASP-Ca^{2+} add-on: 2% $CaCl_2$ and 7% M-ASP.

The burnt areas of the residues from the burning tests of COT/M-ASP and COT/M-ASP-Ca^{2+} samples were analyzed by SEM (Figure 10). In both cases the texture of the cotton fabrics was preserved, despite the burning, thanks to the presence of the PAA coating, which remained intact. At the same time, the cotton fibers appeared partially consumed internally. It should be noted that the surface of COT/M-ASP-Ca^{2+} exhibited some partially exploded bubbles due to the intumescence of M-ASP.

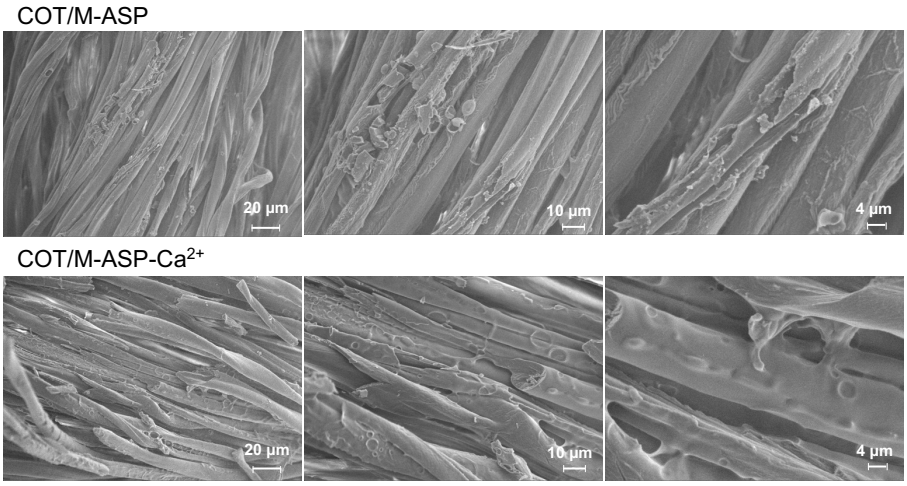

Figure 10. SEM micrographs at different magnifications of the black portion of the combustion residues of COT/M-ASP and COT/M-ASP-Ca^{2+}samples at the end of HFSTs (Figure 9).

3.7.2 Vertical Flame Spread Tests (VFSTs)

The combustion behavior of M-ASP-Ca^{2+}-treated cotton fabrics was also studied by vertical flame spread tests and compared with those of M-ASP-treated cotton fabrics and untreated cotton. Snapshots taken at the beginning and at the end of the combustion are shown in Figure 11. Relevant combustion data are listed in Table 4. Combustion tests performed in vertical configuration are more drastic than those performed in horizontal configuration, as evidenced by the fact that cotton burned much faster (80 s *vs.* 20 s in the presence of flame in VFSTs and HFSTs, respectively). Not unexpectedly, considering the results of HFSTs, $CaCl_2$ failed to inhibit cotton combustion, whereas M-ASP, in line with what previously found (Beduini et al. 2021), weakly protected cotton from combustion, as evidenced by the RMF values reported in Table 4, but was unable to suppress the flame. In contrast, COT/M-ASP-Ca^{2+} did not ignite, showing only a modest afterglow for 35 s, a negligible burned area (Figure 11), and an RMF of approximately 100% (Table 4).

Analogously to what has already been observed in the HFSTs, the mechanism as a flame-retardant of the M-ASP/Ca^{2+} system can be ascribed to the catalytic action of the Ca^{2+} ions on M-ASP carbonization which occurs thanks to the strong interactions between the two species (Figures 3a-3c). In this drastic configuration due to the chimney effect during combustion, the synergism between M-ASP and the Ca^{2+} ions is even greater as cotton ignition is completely inhibited, while in the horizontal configuration cotton ignites, but only burns for a few seconds (flaming combustion time of 3 s, Table 3).

Furthermore, it can be observed that, in VFSTs, Ca^{2+} ions allowed to suppress the combustion of cotton impregnated with both M-ASP and M-GLY, although both PAAs failed in suppressing the flame in these tests, even at much higher add-ons.

However, significant differences were identified in the behavior of the two PAA/$CaCl_2$ formulations, which suggested a greater efficacy of M-ASP compared to M-GLY in interacting with cotton in the presence of Ca^{2+}. The first observation is that the minimum effective add-on was lower for M-ASP than for M-GLY (12% *vs*. 19%, respectively). At 12% add-on, COT/M-ASP-Ca^{2+} did not ignite, whereas COT/M-GLY-Ca^{2+} did at 19% add-on, although the flame extinguished after 5 sec. Secondly, the afterglow flaming time observed with COT/M-ASP-Ca^{2+} was lower than with M-GLY-Ca^{2+} (35 s *vs*. 90 s, respectively). Finally, a lower RMF was obtained with M-GLY-Ca^{2+} compared to M-ASP-Ca^{2+} (82% *vs*. 100%, respectively).

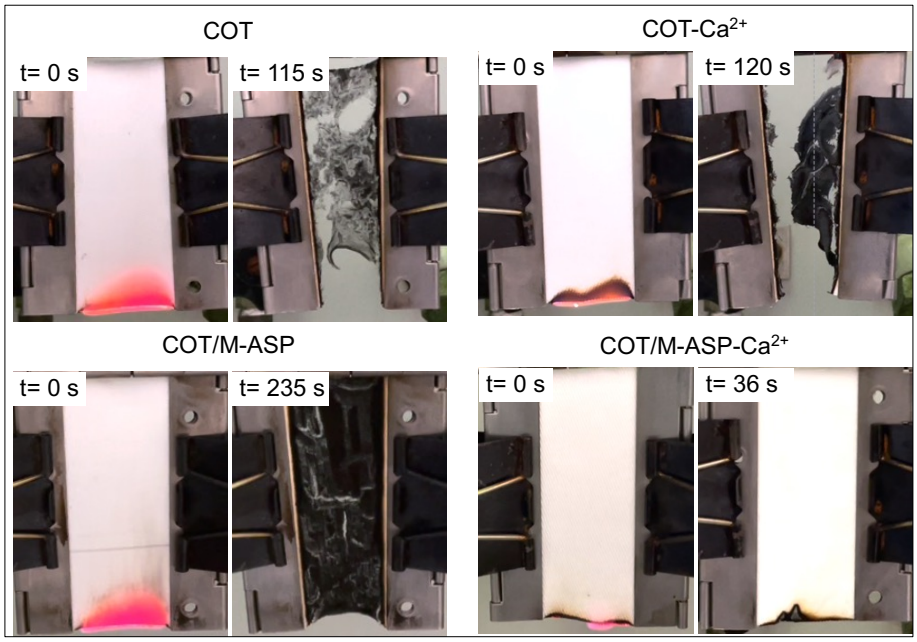

Figure 11. Snapshots of vertical flame spread tests for untreated cotton and cotton treated with Ca^{2+}, M-ASP, and M-ASP-Ca^{2+}. COT/Ca^{2+} add-on: 2%. COT/M-ASP add-on: 12%. COT/M-ASP-Ca^{2+} add-on: 2% $CaCl_2$ and 12% M-ASP.

Table 4. Combustion data of ASP and M-ASP-Ca^{2+}-treated cotton fabrics from vertical flame spread tests.

Sample	Flaming combustion time [a] (s)	Afterglow combustion time [a] (s)	Ignition	RMF [b] (%)
COT	20	32	YES	<1
COT-Ca^{2+} [c]	12	65	YES	5
COT/M-ASP [d]	14	221	YES	22
COT/M-ASP-Ca^{2+} [e]	-	35	NO	~ 100

[a] Combustion time ± 1 s. [b] RMF ± 1.0%. [c] COT/Ca^{2+} add-on: 2%. [d] COT/M-ASP add-on: 12%. [e] COT/M-ASP-Ca^{2+} add-on: 2% $CaCl_2$ and 12% M-ASP.

3.7.3 Oxygen-consumption cone calorimetry tests

Cotton fabrics treated with M-ASP and M-ASP-Ca^{2+} were exposed to a 35 kWm^{-2} heat flux in an oxygen-consumption cone calorimetry. In this experimental condition the sample surface to approximately 520 °C (Schartel et al. 2006). Combustion parameters such as time to ignition (TTI), heat release rate peak (pkHRR), total heat release (THR), and residual mass fraction (RMF) were reported in Table 5. Figure 12 shows the heat release rate (HRR) curves of COT, COT-Ca^{2+}, COT/M-ASP and COT/M-ASP-Ca^{2+}. Both M-ASP and M-ASP-Ca^{2+} significantly affected cotton combustion, reducing its TTI by almost 50%. This can be ascribed to the anticipated formation of thermally stable chars that protect cotton from combustion, reducing the pkHRR by almost 40%. $CaCl_2$ was found efficient as well as M-ASP in terms of pkHRR reductions. It may be observed that the pKHRR reductions were comparable to those of M-GLY, but in the case of M-ASP-Ca^{2+} the M-ASP add-on was lower than with M-GLY (12% *vs*. 19%, respectively) (Alongi et al. 2023).

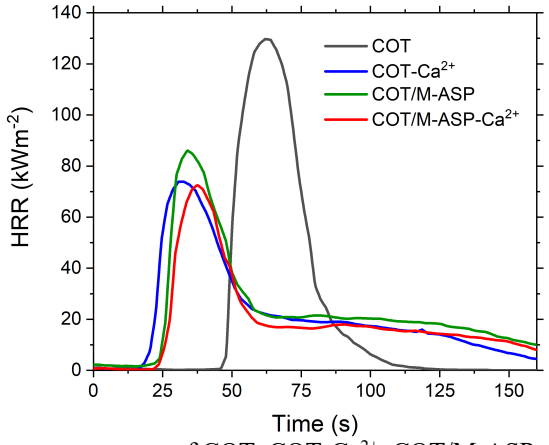

Figure 12. Heat release rate curves of COT, COT-Ca^{2+}, COT/M-ASP and COT/M-ASP-Ca^{2+}. $CaCl_2$ add-on: 2%. M-ASP add-on: 12%. COT/M-ASP-Ca^{2+} add-on: 2% $CaCl_2$ and 12% M-ASP.

Table 5. Combustion data of M-ASP and M-ASP-Ca^{2+}-treated cotton fabrics from oxygen-consumption cone calorimetry.

Sample	**TTI** [a] **(s)**	**pkHRR** [b] **(kWm^{-2}), *(reduction, %)***	**THR** [c] **(MJm^{-2})**	**RMF** [d] **(%)**
COT	50±3	130±2	3.3±0.4	0
COT-Ca^{2+} [e]	26±2	77±10 *(-41%)*	3.2±0.1	3±1
COT/M-ASP [f]	28±7	82±9 *(-37%)*	3.6±0.5	4±1
COT/M-ASP-Ca^{2+} [g]	28±3	77±14 *(-41%)*	3.1±0.3	9±1

[a] TTI: time to ignition. [b] pkHRR: heat release rate peak. [c] THR: total heat release. [d] RMF: residual mass fraction. [e] $CaCl_2$ add-on: 2%. [f] M-ASP add-on: 12%. [g] COT/M-ASP-Ca^{2+} add-on: 2% $CaCl_2$ and 12% M-ASP.

4. Conclusions

In previous work, the PAA derived from the polyaddition of N,N'-methylenebisacrylamide with glycine, encoded M-GLY, was shown to protect cotton fabrics from burning in horizontal flame spread

tests, but not in the more drastic vertical flame spread tests. The addition of small amounts of $CaCl_2$ increased the effectiveness of M-GLY as a flame-retardant to such an extent that it suppressed flaming of cotton even in vertical flame spread tests. The underlying hypothesis was that Ca^{2+} ions could establish ionic and Lewis's acid/base interactions with the repeating units of both cellulose and M-GLY thus affecting the thermo-oxidative decomposition of cellulose. This finding prompted to investigate whether Ca^{2+} ions could even more strongly interact with the PAA synthesized by the polyaddition of N,N'-methylenebisacrylamide with aspartic acid, encoded M-ASP, featuring one additional carboxyl pendant per repeat unit with respect to M-GLY.

TG analysis of M-ASP/$CaCl_2$ mixtures with the same composition used in the protective coatings of cotton, carried out in nitrogen and in air, demonstrated that in both atmospheres the M-ASP-Ca^{2+} adducts had much greater thermal stability than M-ASP alone above 350 °C, and left an unexpectedly high RMF_{800} in both atmospheres. As expected, also COT/M-ASP-Ca^{2+} was much more stable than COT/M-ASP in between 350-800 °C in both nitrogen and air. This finding demonstrated that M-ASP and Ca^{2+} interact synergistically with the pyranose rings of cellulose, favoring its dehydration rather than depolymerization, hence protecting cotton from thermal and thermo-oxidative decomposition.

The performance of M-ASP-Ca^2 as flame-retardant for cotton was investigated in different scenarios and compared with that of M-ASP. In horizontal flame spread tests, M-ASP-Ca^{2+} provided an even more effective protective coating than M-ASP, by exhibiting lower flaming and afterglow combustion times as well as residual mass fraction approaching 100%. The effect of $CaCl_2$ on M-ASP-coated cotton was even more evident in vertical flame spread tests, where plain M-ASP at add-on 12% only weakly protected cotton, leaving a residual mass fraction of 20%, whereas the addition of 2% $CaCl_2$ inhibited ignition and left a residual mass fraction approaching 100%. In oxygen-consumption cone calorimetry tests, both M-ASP and M-ASP-Ca^{2+} significantly affected cotton combustion, reducing the heat release rate peak of approximately 40%.

The results reported here confirm the hypothesis that Ca^{2+} ions, by establishing strong interactions with the repeating units of both cellulose and its α-amino acid-derived PAA coatings, significantly improve the thermal oxidative stability of the system. At the same time, they confirm that this favorable effect can be further enhanced by properly designing the structure of the PAA coating. In particular, the presence, in M-ASP, of one more carboxyl group per repeat unit with respect to M-GLY, make the overall charge of the polyelectrolytic PAA coating more anionic at all working pH's, thus facilitating its interaction with Ca^{2+} ions.

From the above results, it is apparent that if from one side the hydrophilicity of α-amino acid-derived PAAs causes their easy washability, from the other side it allows the intimate and homogeneous interaction between cellulose and PAA. This suggests that, to ensure the durability of the PAA

coatings, it could be highly advantageous to covalently graft them onto cotton. Studies in this direction are currently underway (Beduini et al. 2022).

"The authors declare that no funds, grants, or other support were received during the preparation of this manuscript."

Declarations

Ethics approval and consent to participate: not applicable.

Consent for publication: consent for publication was obtained from all authors.

Availability of data and materials: all data generated or analyzed in this work are included in this publication.

Competing interests: I declare that the authors have no competing interests as defined by Springer, or other interests that might be perceived to influence the results and/or discussion reported in this paper.

Funding: not applicable.

Authors' contributions: all authors contributed to the study. J.A. and R.A. contributed to the methodology and investigation P.F. and E.R. wrote the main manuscript and supervised it. J.A. prepared all figures and commented them. All authors reviewed the manuscript.

Acknowledgements: not applicable.

References

Alongi J, Aad R, Manfredi A, Carosio F, Ferruti P, Ranucci E (2023) Use of calcium chloride to enhance the efficacy of polyamidoamines as flame retardants for cotton. Polym Degrad Stabil 215:110428. https://doi.org/10.1016/j.polymdegradstab.2023.110428

Alongi J, Costantini A, Ferruti P, Ranucci E (2022) Evaluation of the eco-compatibility of polyamidoamines by means of seed germination test. Polym Degrad Stab 167:109854. https://doi.org/10.1016/j.polymdegradstab.2022.109854

Barbalini M, Bartoli M, Tagliaferro A, Malucelli G (2020) Phytic acid and biochar: An effective all bio-sourced flame retardant formulation for cotton fabrics. Polymers 12:811. https://doi.org/10.3390/polym12040811

Beduini A, Carosio F, Ferruti P, Ranucci E, Alongi J (2019) Sulfur-based copolymeric polyamidoamines as efficient flame-retardants for cotton. Polymers 11:1904. https://doi.org/10.3390/polym11111904

Beduini A, Ferruti P, Carosio F, Ranucci E, Alongi J (2021) Polyamidoamines derived from natural α-amino acids as effective flame retardants for cotton. Polymers 13:3714. https://doi.org/10.3390/polym13213714

Beduini A, Porta F, Nebbia S, Carosio F, Ranucci E, Ferruti P, Alongi J (2022) Durable, washing resistant flame-retardant finishing for cotton fabrics by covalent grafting of α-amino acid-derived polyamidoamines. Proceedings of the Milan Polymer Days Congress, 19-21 June 2022, Milan, Italy, p. 7, ISBN 978-88-3623-096-9.

Bourbigot S, Le Bras M, Duquesne S, Rochery M (2004) Recent advances for intumescent polymers. Macromol Mater Eng 289:489-511. https://doi.org/10.1002/mame.200400007

Cheng D, Li T, Smith G, Yang J, Hang C, Miao Z, Wu Z (2019) Influence of calcium chloride impregnation on the thermal and high-temperature carbonization properties of bamboo fiber. PLOS ONE 14:1-12. https://doi.org/10.1371/journal.pone.0212886

Davies PJ, Horrocks AR, Alderson A (2005) The sensitisation of thermal decomposition of ammonium polyphosphate by selected metal ions and their potential for improved cotton fabric flame retardancy. Polym Degrad Stabil 88:114-122. https://doi.org/10.1016/j.polymdegradstab.2004.01.029

Diao S, Yang Y, Tang Q, Lu Y, Zhang F (2023) Improvement of traditional proban flame retardant finishing technology for cotton fabric. Cellulose 30:6051-6063. https://doi.org/10.1007/s10570-023-05226-4

Ferruti P (2013) Polyamidoamines: past, present and perspectives. J Polym Sci Polym Chem 51:2319-2353. https://doi.org/10.1002/pola.26632

Ferruti P, Marchisio MA, Duncan R (2002). Poly(amido-amine)s: biomedical applications. Macromol Rapid Commun 23:332-355. https://doi.org/10.1002/1521-3927(20020401)23:5/6<332::AID-MARC332>3.0.CO;2-I

Forte C, Alongi J, Beduini A, Borsacchi S, Calucci S, Carosio F, Ferruti P, Ranucci E (2021) The thermo-oxidative behavior of cotton coated with an intumescent flame retardant glycine-derived

polyamidoamine: a multi-technique study. Polymers 13:4382. https://doi.org/10.3390/polym13244382

Horrocks AR (2011) Flame retardant challenges for textiles and fibres: new chemistry versus innovatory solutions. Polym. Degrad Stabil 96:377-392. https://doi.org/10.1016/j.polymdegradstab.2010.03.036

Horrocks AR (2013) Regulatory and Testing Requirements for Flameretardant Textile Applications. In Alongi J, Carosio F, Horrocks AR, Malucelli G (Eds) Update on Flame Retardant textiles: State of the art, Environmental Issues and Innovative Solutions, Smithers RAPRA, Publishing, Shawbury, Shrewsbury, Shropshire (UK), chapter 3, pp. 53-122 (ISBN:978-1-90903-017-6).

Horrocks AR, Kandola BK, Davies PJ, Zhang S, Padbury SA (2005) Developments in flame retardant textiles – A review. Polym Degrad Stab 33:3-12. https://doi.org/10.1016/j.polymdegradstab.2003.10.024

Islam S, van de Ven TGM (2021) Cotton-based flame retardant textile: a review. BioResources 16:4354-4381. https://doi.org/10.15376/biores.16.2.Islam

ISO 5660 (2002) In Fire Test, Reaction to Fire, Rate of Heat Release (Cone Calorimeter Method); International Organization for Standardization: Geneva, Switzerland.

Kang M, Chen S, Yang R, Li D, Wenchao Z (2022) Fabrication of an eco-friendly clay-based coating for enhancing flame retardant and mechanical properties of cotton fabrics via LbL assembly. Polymers 14:4994. https://doi.org/10.3390/polym14224994

Ling C, Guo L, Wang Z (2023) A review on the state of flame-retardant cotton fabrics: mechanism and applications. Ind Crops Prod 194:116264. https://doi.org/10.1016/j.indcrop.2023.116264

Manfredi A, Carosio F, Ferruti P, Ranucci E, Alongi J (2018) Linear polyamidoamines as novel biocompatible phosphorus-free surface confined intumescent flame retardants for cotton fabrics. Polym Degrad Stabil 151:52-64. https://doi.org/10.1016/j.polymdegradstab.2018.02.020

Morterra C, Low MJD (1983) IR Studies of carbons – II: The vacuum pyrolysis of cellulose. Carbon 21:283-288. https://doi.org/10.1016/0008-6223(83)90092-1

Morterra C, Low MJD (1985) IR Studies of carbons – V: Effects of NaCl on cellulose pyrolisis and char oxidation. Carbon 23:311-316. https://doi.org/10.1016/0008-6223(85)90116-2

Patwardhan P, Satrio J, Brown R, Shanks B (2010) Influence of inorganic salts on the primary pyrolysis products of cellulose. Bioresour Technol 101:4646-4655. https://doi.org/10.1016/j.biortech.2010.01.112

Ponder RG, Richards GN, Stevenson TT (1992) Influence of linkage position and orientation in pyrolysis of polysaccharides: A study of several glucans. J Anal Appl Pyrolysis 22:217-229. https://doi.org/10.1016/0165-2370(92)85015-D

Rietzler B, Manian AP, Rhomberg D, Bechtold T, Pham T (2021) Investigation of the decomplexation of polyamide/$CaCl_2$ complex toward a green, nondestructive recovery of polyamide from textile waste. J Appl Polym Sci 138:e51170. https://doi.org/10.1002/app.51170

Salmeia KA, Gaan S, Malucelli G (2016a) Recent advances for flame retardancy of textiles based on phosphorus chemistry. Polymers 9:319. https://doi.org/10.3390/polym8090319

Salmeia KA, Jovic M, Ragaisiene A, Rukuiziene Z, Milasius R, Mikucioniene D, Gaan S (2016b) Flammability of cellulose-based fibers and the effect of structure of phosphorus compounds on their flame retardancy. Polymers 8:293. https://doi.org/10.3390/polym8080293.

Salmeia KA, Jovic M, Ragaisiene A, Rukuiziene Z, Milasius R, Mikucioniene D, Gaan S (2016c) Flammability of cellulose-based fibers and the effect of structure of phosphorus compounds on their flame retardancy. Polymers 8:293. https://doi.org/10.3390/polym8080293.

Schartel B, Bartholomai M, Knoll U (2006) Some comments on the main fire retardancy mechanisms in polymer nanocomposites. Polym Adv Technol 17:772-777. https://doi.org/10.1002/pat.792

Sekiguchi Y, Frye JS, Shafizadeh F (1983) Structure and formation of chars. J Appl Polym Sci 28:3513-3525. https://doi.org/10.1002/app.1983.070281116

Sekiguchi Y, Shafizadeh F (1984) The effect of inorganic additives on the formation, composition, and combustion of cellulosic char. J Appl Polym Sci 29:1267-1286. https://doi.org/10.1002/app.1984.070290421

Shafizadeh F, Fu YL (1973) Pyrolysis of cellulose. Carbohydr Research 29:113-122. https://doi.org/10.1016/S0008-6215(00)82074-1

Shafizadeh F, Sekiguchi Y (1983) Development of aromaticity in cellulose chars. Carbon 21:511-516. https://doi.org/10.1016/0008-6223(83)90144-6

Speece J, EC74-492 Fabric Flammability and Clothing. University of Nebraska - Lincoln DigitalCommons@University of Nebraska - Lincoln, 1974.

Sun L, Wang H, Li W, Zhang J, Zhang Z, Lu Z, Zhu P, Dong C (2021) Preparation and characterization and testing of flame retardant cotton cellulose material: flame retardancy, thermal stability and flame-retardant mechanism. Cellulose 28:3789-3805. https://doi.org/10.1007/s10570-020-03632-6

Sun L, Xie Y, Wu J, Wang H, Wang S, Li W, Zhang J, Zhang Z, Zhu P, Lu Z, Dong C A novel P/N (2021) Flame retardant synthesized by one-step method towards cotton materials and its flame-retardant mechanism. Cellulose 28:3249-3264. https://doi.org/10.1007/s10570-021-03728-7

Tata J, Alongi J, Carosio F, Frache A (2011) Optimization of the procedure to burn textile fabrics by cone calorimeter: Part I. Combustion behavior of polyester. Fire Mater 35:397-409. https://doi.org/10.1002/fam.1061

Tian CM, Guo HZ, Zhang, Xu JZ, Shi JR (1995) Study on the thermal degradation of cotton cellulose ammonium phosphate and its metal complexes. Thermochim Acta 253: 243-251. https://doi.org/10.1016/0040-6031(94)02081-X

Tian CM, Xie JX, Guo HZ, Xu JZ (2003) The effect of metal ions on thermal oxidative degradation of cotton cellulose ammonium phosphate. J Thermal Anal Calorim 73:827-834. https://doi.org/10.1023/A:1025838732084

Varhegyi G, Antal MJ, Szekely T, Till F, Jakab E (1988) Simultaneous thermogravimetric–mass spectrometric studies of the thermal decomposition of biopolymers. 1. Avicel cellulose in the presence and absence of catalysts. Energy Fuels 2:267-272. https://doi.org/10.1021/ef00009a007

Xia L, Lv Y, Miao Z, Luo L, Luo W, Xu Y, Yuan C, Zeng B, Dai L (2022a) A flame retardant fabric nanocoating based on nanocarbon black particles@polymer composite and its fire-alarm application. Chemical Eng J 433:133501. https://doi.org/10.1016/j.cej.2021.133501

Xia L, Dai J, Wang X, Xue M, Xu Y, Yuan C, Dai L (2022b) Facile fabrication of multifunctional cotton fabric by AgNC@boronate polymer/crosslinked chitosan. Carbohydr Polym 288:119384. https://doi.org/10.1016/j.carbpol.2022.119384

Xu F, Zhong L, Xu Y, Zhang C, Zhang F, Zhang G (2019) Highly efficent flame-retardant and soft cotton fabrics prepared by a novel reactive flame retardant. Cellulose 26:4225-4240. https://doi.org/10.1007/s10570-019-02374-4

Yu Y (2013). Formation and characteristics of reaction intermediates from the fast pyrolysis of NaCl- and $MgCl_2$-loaded celluloses. Energy Fuels 28:245-253. https://doi.org/10.1021/ef401483u

Zilke O, Plohl D, Opwis K, Mayer-Gall, T, Gutmann, JS (2020) A flame-retardant phytic-acid-based LbL-coating for cotton using polyvinylamine. Polymers 12:1202. https://doi.org/10.3390/polym12051202